



Internal States Influence the Representation and Modulation of Food Intake by Subthalamic Neurons

Haichuan Wu¹ · Xiang Yan¹ · Dongliang Tang¹ · Weixin Gu¹ · Yiwen Luan¹ · Haijiang Cai³ · Chunyi Zhou^{1,2} · Cheng Xiao^{1,2} 

Received: 22 December 2019 / Accepted: 16 February 2020 / Published online: 21 June 2020
© Shanghai Institutes for Biological Sciences, CAS 2020

Abstract Deep brain stimulation of the subthalamic nucleus (STN) is an effective therapy for motor deficits in Parkinson's disease (PD), but commonly causes weight gain in late-phase PD patients probably by increasing feeding motivation. It is unclear how STN neurons represent and modulate feeding behavior in different internal states. In the present study, we found that feeding caused a robust activation of STN neurons in mice (GCaMP6 signal increased by $48.4\% \pm 7.2\%$, $n = 9$, $P = 0.0003$), and the extent varied with the size, valence, and palatability of food, but not with the repetition of feeding. Interestingly, energy deprivation increased the spontaneous firing rate (8.5 ± 1.5 Hz, $n = 17$, versus 4.7 ± 0.7 Hz, $n = 18$, $P = 0.03$) and the depolarization-induced spikes in STN neurons, as well as enhanced the STN responses to feeding. Optogenetic experiments revealed that stimulation and inhibition of STN neurons respectively reduced (by $11\% \pm 6\%$, $n = 6$, $P = 0.02$) and enhanced (by $36\% \pm 15\%$, $n = 7$, $P = 0.03$) food intake only in the dark phase. In conclusion, our results support the hypothesis that STN neurons are activated by feeding behavior, depending on energy

homeostatic status and the palatability of food, and modulation of these neurons is sufficient to regulate food intake.

Keywords Subthalamic nucleus · Food intake · Fiber photometry · Optogenetics

Introduction

Accumulating investigations demonstrate that deep brain stimulation (DBS) in the STN, an efficient therapy for cardinal motor symptoms in Parkinson's disease (PD) [1–3], commonly increases the patients' weight [4–10]. Some studies support the idea that STN DBS-induced weight gain may result from off-target stimulation of neighboring nuclei, including the lateral hypothalamus, altering the release of feeding-related hormones [11–15]. But, some PD patients gain weight when the DBS electrode leads are in the STN and feeding-related hormones are normal [16, 17]. As DBS inhibits the activity of STN neurons [1, 2, 18], the weight gain following STN DBS in PD patients may be associated with the inhibition of STN neurons. Consistent with this notion, increased motivation for food intake has been reported in patients with strokes or tumors involving the STN [19, 20] and in rats subjected to STN lesions [21, 22]. In fact, STN DBS is unable to selectively regulate STN neurons while leaving neighboring axons unperturbed, and both physical and chemical lesions of the STN may cause neuroadaptation. These limitations may complicate the understanding of whether and how STN neurons modulate food intake.

Food intake is primarily governed by feeding circuits comprised of hormones, including leptin, ghrelin, insulin, and neuropeptide Y acting on hypothalamic and brainstem

Haichuan Wu, Xiang Yan and Dongliang Tang have contributed equally to this work.

✉ Chunyi Zhou
chunyi.zhou@xzhmu.edu.cn

✉ Cheng Xiao
xchengxj@xzhmu.edu.cn

¹ School of Anesthesiology, Xuzhou Medical University, Xuzhou 221004, China

² Jiangsu Province Key Laboratory of Anesthesiology, Xuzhou Medical University, Xuzhou 221004, China

³ Department of Neuroscience, University of Arizona, Tucson, AZ 85721, USA

nuclei [23–25]. The levels of these hormones fluctuate with energy homeostasis to drive the initiation and termination of feeding [26, 27]. In addition, reward pathways convey ‘liking’ or ‘wanting’ less or sufficiently palatable food, and strongly alter food intake [23, 24, 26, 28]. Evidence has implicated the STN in reward processing [29–31]. For instance, the activity of STN neurons is enhanced when animals obtain a liquid reward, and discriminate the valence of the reward; after Pavlovian conditioning is established, STN neurons also respond to reward expectation and omission [29, 30]. But these studies did not explore the STN responses to solid foods with different palatability in hungry or sated animals, which is important for characterizing the involvement of the STN in feeding behaviors.

To measure neuronal activity, we labeled STN neurons with AAV viral vector carrying the genetically-encoded Ca^{2+} sensor GCaMP6 for fiber photometric recordings [32]. As DBS recruits multiple components in the STN [2], including afferent, efferent, and *en passant* fibers, as well as nearby neurons, to elucidate the potential effects of STN neurons on food intake, we applied optogenetics to achieve the bidirectional modulation of STN neurons [18]. Our results suggested that STN neurons are not only activated by feeding, varying with the energy status of mice and the size, valence, and palatability of the food, but also regulate food intake during the active state (dark phase). This could be a physiological mechanism underlying the weight gain following STN DBS.

Materials and Methods

The care and use of animals and the experimental protocols of this study were approved by the Institutional Animal Care and Use Committee and the Office of Laboratory Animal Resources of Xuzhou Medical University, following the National Institutes of Health Guide for the Care and Use of Laboratory Animals (NIH Publication No. 8023, revised 1978). C57BL/6 mice were purchased from Jinan Pengyue Laboratory Animal Breeding Co., Ltd (Jinan, China), and were group-housed (≤ 4 per cage) on a 12-h light/dark cycle. The mice had free access to water and food. In some feeding experiments, the mice were fasted using paradigms described in the Results. Efforts were made to minimize animal suffering and to reduce the number of animals used.

Animal Surgery

Mice (4–5 months old) were anesthetized with sodium pentobarbital (40 mg/kg) and stabilized on a stereotaxic frame (RWD Life Science Co., Ltd, Shenzhen, China).

Adeno-associated viral vector serotype 2 (AAV2/9) carrying CaMKII promoter-driven GCaMP6S or Chr2-eYFP or NpHR3.0-eYFP or eGFP ($0.3 \mu\text{L}$, $2\text{--}4 \times 10^{12}$ viral genome copies/mL, BrainVTA (Wuhan) Co. Ltd, Wuhan, China) was injected into the STN (AP, 1.75 mm; ML, 1.5 mm; DV, 4.8 mm). Then, we bilaterally implanted optical fibers (200 μm in diameter, NA 0.37; Inper, Hangzhou, China) with tips at the viral injection site for fiber photometric recordings, or at 0.2 mm above this site for optogenetic modulation. The mice were allowed 4 weeks of recovery before the experiments.

Patch-Clamp Recordings

To verify the function of the viral vectors used for fiber photometry and optogenetic manipulations, we performed patch-clamp recordings on brain slices prepared from 5–7-month old C57BL/6 (wild-type, WT) mice, using a previously described protocol with some modifications [32–35]. In brief, the mice were deeply euthanized with CO_2 , and then decapitated. The brain was removed and cut into parasagittal slices on a vibratome (VT-1200S, Leica, Wetzlar, Germany) while immersed in ice-cold modified sucrose-based artificial cerebrospinal fluid (sACSF) (containing (mmol/L) 85 NaCl, 75 sucrose, 2.5 KCl, 1.25 NaH_2PO_4 , 4.0 MgCl_2 , 0.5 CaCl_2 , 24 NaHCO_3 and 25 glucose) saturated with 95% O_2 /5% CO_2 (carbogen) [32]. Slices containing the STN were allowed to recover at $32 \pm 1^\circ\text{C}$ in a holding chamber, filled with carbogenated sACSF. One hour later, the slices were transferred into carbogenated normal ACSF, containing (mmol/L) 125 NaCl, 2.5 KCl, 1.2 NaH_2PO_4 , 1.2 MgCl_2 , 2.4 CaCl_2 , 26 NaHCO_3 , and 11 glucose, and kept at room temperature. One slice was transferred into the recording chamber, and superfused (1.5–2.0 mL/min) with carbogenated ACSF at $32 \pm 0.5^\circ\text{C}$. Three to four slices per mouse were used for recordings on each day.

The neurons in slices were visualized under an upright microscope (FN-1, Nikon, Tokyo, Japan) equipped with a CCD-camera (Hamamatsu Flash 4.0 LTE, Iwata, Japan) and near-infrared and green fluorescence illumination. Whole-cell patch-clamp techniques were used to record electrophysiological signals with MultiClamp 700B amplifiers (Molecular Devices, San Jose, USA), Digidata 1550B analog-to-digital converter (Molecular Devices, San Jose, USA), and pClamp 10.7 software (Molecular Devices, San Jose, USA). Each patch electrode had a resistance of 4–6 $\text{M}\Omega$ when filled with pipette solution containing (in mmol/L) 135 K gluconate, 5 KCl, 0.2 EGTA, 0.5 CaCl_2 , 10 HEPES, 2 Mg-ATP, and 0.1 GTP. The pH of the solutions was adjusted to 7.2 with Tris-base, and the osmolarity was adjusted to 300 mOsm with sucrose.

Blue (472 nm) and yellow (589 nm) light (Doric lens LED fiber light sources: 4-channel model, Quebec, Canada) were delivered to STN neurons expressing ChR2-eYFP and NpHR3.0-eYFP, and the light responses of these neurons were recorded in both voltage- and current-clamp modes.

Fiber Photometry

The mice receiving AAV2-CaMKII-GCaMP6S or AAV2-CaMKII-eYFP injection and carrying an optical implant with the tip in the STN were transferred to a testing room. After an hour of habituation to the environment, each mouse was placed in a narrow track or a clean cage. Fiber photometry instrument (Thinkertech, Nanjing, China) [36–39] was used to monitor the GCaMP6 signals in STN neurons, and the mouse was simultaneously monitored with an animal behavior tracking system (Noldus Information Technology, Wageningen, The Netherlands) through an infra-red camera. We adjusted the instrument by setting the excitation light to 50 μ W and the gain to a level that gave a background signal of 3 units measured when the end of the input cable was in the dark. After the input cable was connected to the optical implant in the mouse, the instrument read total light signals. The difference between the total signal and the background signal was used as the baseline GCaMP6 signal. To quantify responses evoked by eating or drinking, we averaged the GCaMP6 signal during 2 s just before the response to give the F_0 value. The peak response was quantified as $[\text{peak signal (F)} - F_0] \times 100\% / F_0$ (in the figures, $(F - F_0)$ is abbreviated to ΔF). The total response of STN neurons to one eating bout was quantified as the area under the peak (unit \times s), that is, the area under the curve (AUC).

Optogenetic Modulation of STN Neurons

The mice receiving AAV2-CaMKII-ChR2-eYFP injection and carrying an optical implant with the tip in the STN were used for the optogenetic stimulation of STN neurons, while those receiving AAV2-CaMKII-NpHR3.0-eYFP injection in the STN were used for optogenetic inhibition. The mice receiving AAV2-CaMKII-eGFP served as controls. Blue (473 nm, 5 ms pulses, 4 mW) and yellow (598 nm, constant, 3.5 mW) lasers (Newdoon, Hangzhou, China) were used to activate ChR2 and NpHR3.0, respectively *in vivo*. After experiments, each mouse was euthanized in a CO₂ chamber, and the location of optical implant and viral expression and spread were checked under a fluorescence microscope. Mice with off-target implants, poorly-expressed virus, or spread of virus to other areas were excluded.

Behavioral Tests

Food Intake

Before the experiments, we provided peanut pellets, small chocolate chunks, and sugar bars to mice for 1 h each day for 3 consecutive days to familiarize them with these palatable foods. The small pieces of these foods and rodent chow weighed 20 mg–60 mg, and the mice were able to consume each piece of food in a single bout. Food intake was measured after the specific feeding paradigms described in the Results.

Voluntary Movement Test

Mice were placed in a round open field arena and their motor behavior was recorded with a video camera controlled by Ethovision XT 11.5 software (Noldus Information Technology, Wageningen, The Netherlands) [33, 40]. After a 10-min baseline measurement, the mice were subjected to 3 min optogenetic stimulation or inhibition of STN neurons. The distances traveled were compared before and during optogenetic modulation to address whether the motor functions were altered.

Confocal Microscopy

Low and high magnification images were acquired with a Zeiss LSM 880 confocal microscope (Oberkochen, Germany), equipped with Plan Apochromat air objectives [10 \times (NA, 0.45), 20 \times (NA, 0.8), and 40 \times (NA, 0.95)] and six laser lines (405, 458, 488, 512, 561, and 633 nm). The microscope was controlled by Zen2 acquisition software (Zeiss, Oberkochen, Germany), enabling automatic tiling and z-stacking. The images were processed with ImageJ [41].

Data Analysis

The fiber photometry signals were converted into Excel files with a program provided by the manufacturer (Thinkertech, Nanjing, China), then were read and processed in Clampfit 10.7 (Molecular Devices). The event-related responses of GCaMP6 signals were quantified as the peak over the baseline, and are presented as percentage changes. The two-tailed paired *t*-test or the Wilcoxon signed-rank test was used to analyze the differences of STN responses and food consumption under different conditions. One-way ANOVA was used to compare STN responses to different types of palatable food. Repeated measures ANOVA was used to analyze the changes of STN responses to repeated consumption of foods. *P* values <0.05 were regarded as statistically significant.

Results

STN Neurons Respond to Food Consumption in Freely-Moving Mice

To address whether STN neurons are involved in mouse feeding behavior, we used fiber photometry to examine the change of STN neuronal activity when the mice were consuming food (Fig. 1A, B). During feeding tests, we kept a mouse outside the sliding gate to a track, while placing a piece of peanut pellet by the end of the track (Fig. 1B). Interestingly, we recorded a robust rise in the GCaMP6S signal in the STN when a mouse grabbed and ate a peanut pellet, and the signal returned to baseline after the mouse finished eating (Fig. 1C, left panel). The durations of GCaMP6S signal bursts matched those of eating bouts. Because of the fast decay, the STN responses likely derived from the actions of ingestion, including licking, biting, chewing, and swallowing, and the feelings related to these actions. The fluorescence signal in the STN transduced with eYFP remained the same when a mouse was eating a peanut pellet (Fig. 1C, right panel, D, E). After finishing the behavioral tests, we sacrificed the mice and confirmed that the optical fibers were localized in the STN (Fig. 1B, right panel). The data indicated that STN neurons respond to food consumption.

To determine whether the response of STN neurons to food diminishes with repetitive consumption, we used two paradigms: 5 trials with an interval of 1 min (Fig. 1F, G), and 5 trials with an interval of 1 min on 5 consecutive days (Fig. 1H, I). We found that the food consumption-induced increase of the GCaMP6S signal did not change with repetitive feeding in the two paradigms.

When we randomly fed the mice with 30, 50, or 90 mg peanut pellets, the mice ate the pellets within a single eating bout. The durations of the eating bouts increased with pellet size (Fig. 1J). The STN responses to peanut consumption displayed similar amplitudes, but increased durations as pellet size increased (Fig. 1J, K, L), consistent with the notion that the STN responses concord with eating bouts.

Motivation to meet physiological homeostasis is one of the major drives for animals to eat and drink. Mice may evaluate the outcome after finishing the action of biting and drinking. To address whether STN neurons encode the action or evaluation of the outcome of the action, we provided the mice with artificial food, a piece of rubber with the shape of rodent chow. When we compared the STN responses to artificial food and real rodent chow (Fig. 2A), we found that the biting (without eating) of artificial food resulted in much smaller responses in STN neurons than those of rodent chow (Fig. 2B, C), and the

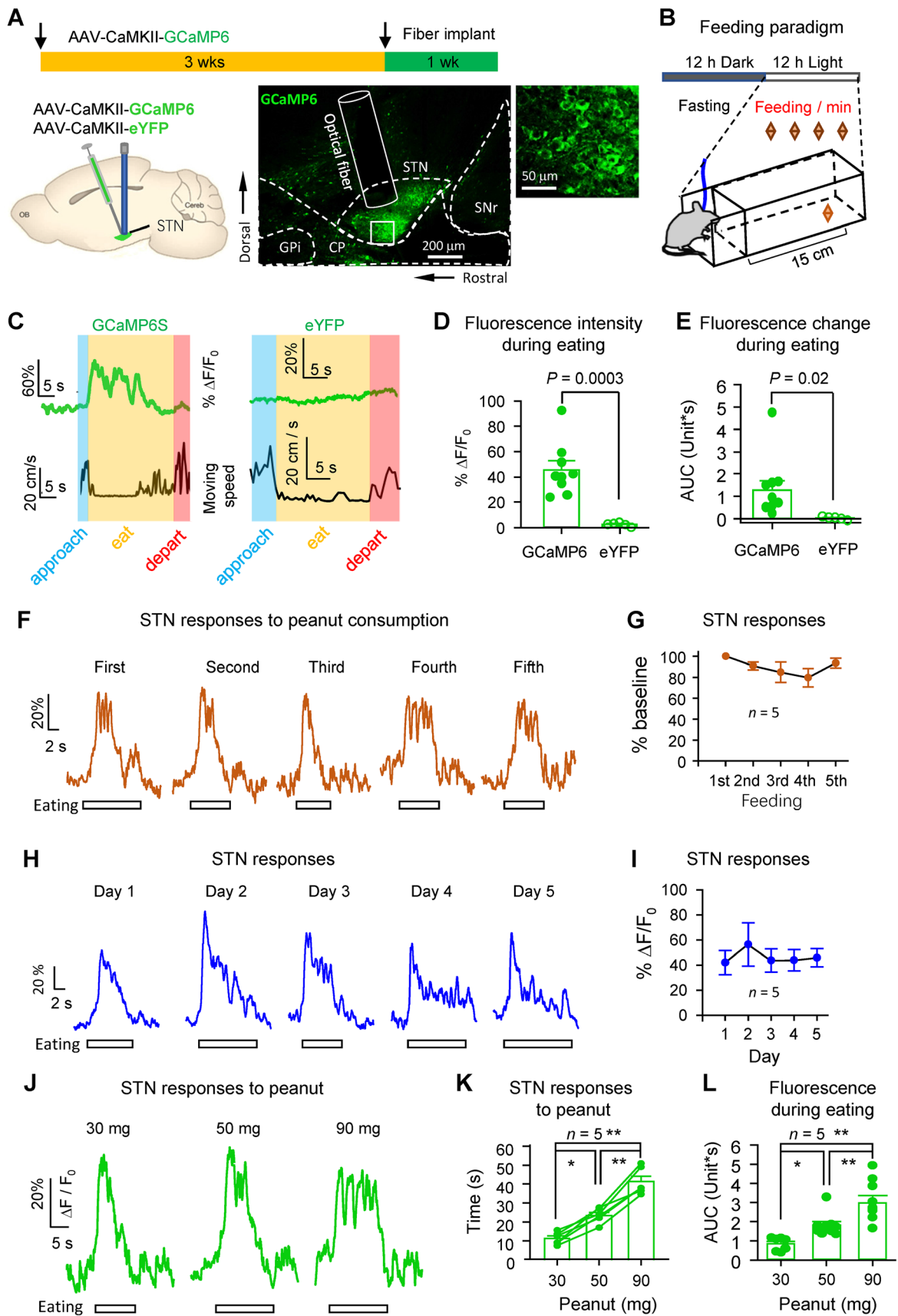
Fig. 1 The activity of STN neurons is enhanced during food consumption. **A** Schematic of recording protocol. Left panel, AAV-CaMKII-GCaMP6S or AAV-CaMKII-eYFP was injected into the STN to infect STN neurons; middle panel, a 200- μ m optical fiber was inserted into the STN to record GCaMP6 signals; right panel, higher magnification image corresponding to the white box under the optical fiber (cp, cerebral peduncle; GPI, internal segment of the globus pallidus; SNr, substantia nigra pars reticulata). **B** Cartoon of feeding paradigm. Mice fasted overnight are placed in a narrow chamber behind a sliding gate, and food is provided 15 cm from the gate. **C** GCaMP6S and eYFP signal (green trace) in STN neurons and moving speed (black trace) were aligned when the mouse approached the food pellet, ate it, and departed. **D**, **E** Summary of changes in GCaMP6S ($n = 9$) and eYFP signal ($n = 9$) in the STN in response to food consumption (peak: $t = 6.12$, $P = 0.0003$, two-tailed t -test; area under the curve (AUC): $t = 2.95$, $P = 0.02$, two-tailed t -test). **F**–**I** Typical amplitudes (**F**) and summary (**G**) of STN responses to food consumption on the same day ($n = 6$, $F = 1.29$, $P = 0.31$, repeated measures ANOVA) and on consecutive days (**H** and **I**) ($n = 6$, $F = 1.29$, $P = 0.31$, repeated measures ANOVA). **J**, **K** Typical durations (**J**) and summary (**K**) of responses of STN neurons to food pellets of different sizes ($F = 146.4$, $P < 0.001$, repeated measures ANOVA, pairwise multiple comparisons, $P < 0.001$, Student-Newman-Keuls method). **L** Summary of AUC ($F = 17.81$, $P < 0.001$, one-way ANOVA).

difference may correspond to the outcome evaluation after food reception.

We also examined the responses of STN neurons to licks of a water nozzle with or without the delivery of water in mice being deprived of water for 12 h in the dark phase (Fig. 2D). We found GCaMP6S peaks in STN neurons congruent with bouts of licking, and the responses were larger when water was provided (Fig. 2E, F). Consistent with those to food consumption (Fig. 1F, G), the peak responses of STN neurons to bouts of licking with or without water did not change in consecutive trials (Fig. 2G). These data suggest that STN neurons might enhance activity not only upon actions to obtain food and water, but also upon outcome evaluation after the reception of food and water.

Effects of Palatability and Aversive Flavor of Foods on STN Responses in Hungry Mice

We then performed experiments to determine whether the food responses of STN neurons differ with the food properties: palatability (Fig. 3A) and aversive flavor (Fig. 3C). As the rewarding effects of a food may vary with its palatability, we fed hungry mice with rodent chow and palatable foods (such as sugar, peanut and chocolate) to determine whether STN neurons respond differently. Before the tests, we exposed the mice to 5–10 pellets of these palatable foods each day for 2–3 consecutive days to familiarize them with the foods. This procedure may eliminate the confounding effects of food familiarity on the



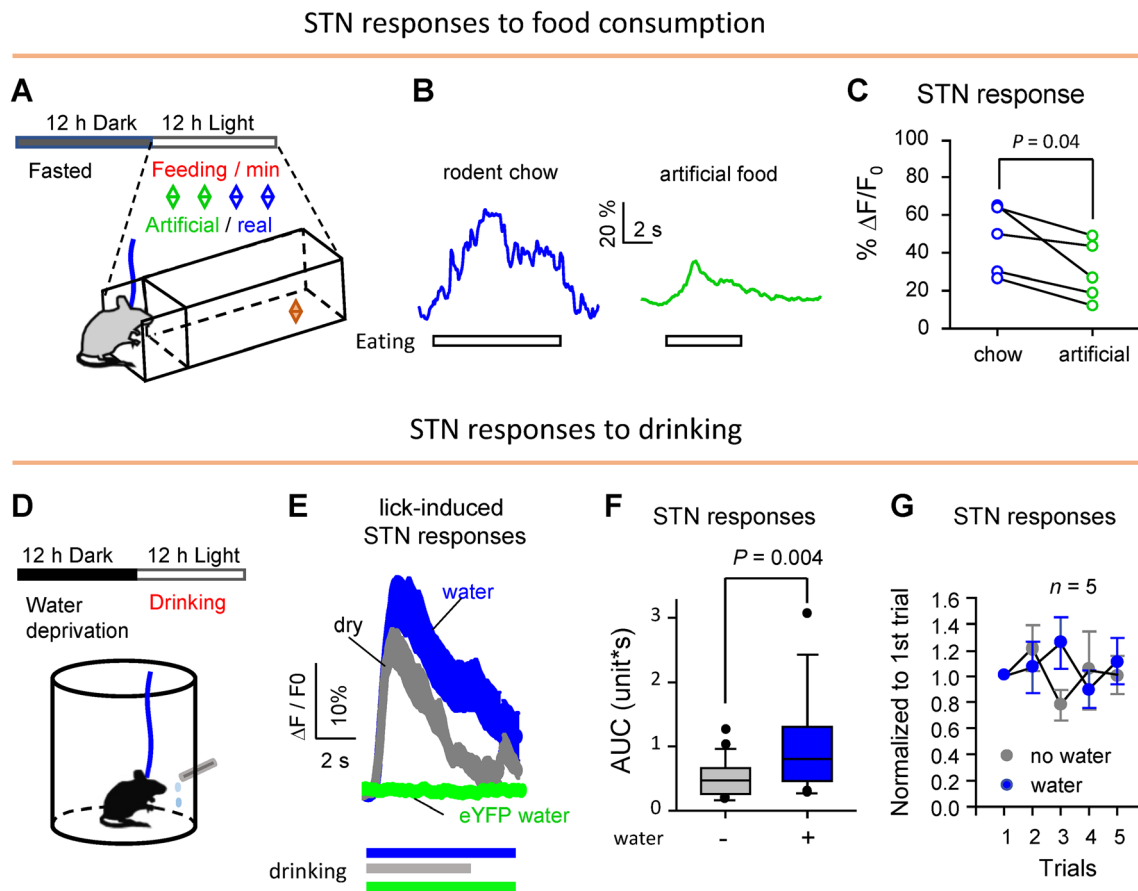


Fig. 2 STN neurons are activated by both the procurement and outcome evaluation of food. **A** Cartoon of feeding paradigm. After fasting, mice were presented with rodent chow or artificial food. **B**, **C** Typical (**B**) and summary responses (**C**) of STN neurons to rodent chow and artificial food ($n = 5$, $t = 3.1$, $P = 0.04$, paired t -test). **D** Cartoon of drinking paradigm. After overnight deprivation of water each mouse is allowed to drink from a water nozzle in which the water flow is controlled by an electromagnetic valve. **E** Licking responses in STN neurons recorded when water is (blue) or is not

(gray) delivered (mean \pm SEM). **F** Box plots of the AUC of licking responses of STN neurons ($T = 350$, $P = 0.004$, Mann-Whitney rank sum test). Each trace represents a response of STN neurons to a bout of licks. Twenty-five traces (5 traces from each of 5 mice) are summarized in **E** and **F**. **G** Amplitudes of STN responses to licks with ($F = 1.18$, $P = 0.36$, one-way repeated measures ANOVA) and without ($F = 2.67$, $P = 0.10$, one-way repeated measures ANOVA) water *versus* trial number.

results. We found that the GCaMP6S signal in STN neurons increased with similar amplitudes when the mice were consuming these foods (Fig. 3A, B). Therefore, in the hungry state, STN neurons may not discriminate the palatability of foods.

To determine whether STN neurons also respond to aversive signals, we provided the mice with bitter peanut pellets (dipped in 0.2% quinine) (Fig. 3C). They usually did not eat up the bitter peanut pellet within a single eating bout. Thus, the duration of each bout was much shorter than that for a plain peanut pellet (Fig. 3C). The STN neurons showed much shorter and smaller responses to the consumption of bitter peanuts than to plain peanuts (Fig. 3C, D, E).

The STN responses to the plain and bitter peanut pellets suggest that STN neurons may encode the valence of the food with varied enhancement in activity.

Satiation Reduces the Responses of STN Neurons to Food Consumption

It is well known that feeding behaviors are regulated by the status of energy homeostasis [23, 26, 27]. We next compared STN responses to food consumption in mice after overnight fasting or after feeding *ad libitum* in the dark phase (Fig. 4A). Although immediately after entering the track the mice directly approached food at similar speeds in both hungry and sated states (Fig. 4B), they consumed less pellets of chocolate, peanut, and rodent chow after they were regularly fed (Fig. 4C). These results are consistent with the notion that sated mice have a reduced appetite. Furthermore, the enhancement of STN neuronal activity recorded with fiber photometry in response to the consumption of chocolate, peanut, and rodent chow was attenuated when the mice were regularly

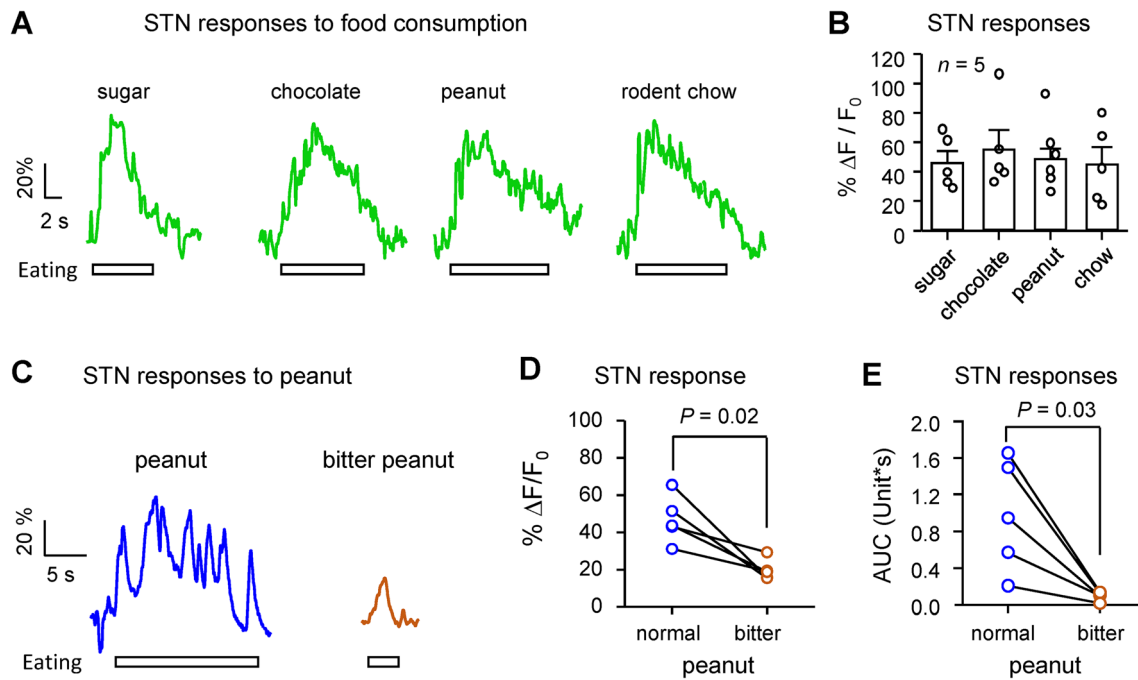


Fig. 3 The responses of STN neurons to consumption of palatable and bitter foods after an overnight fast. **A–B** Typical responses (**A**) and summary of responses (**B**) of STN neurons to sugar, chocolate, peanut, and rodent chow ($n = 5$, $H = 0.65$, $P = 0.89$, Kruskal-Wallis one-way analysis of variance on ranks). **C–**

fed (Fig. 4D, E). Therefore, satiation reduces the STN responses to food consumption.

In addition, in sated mice, STN responses to consumption of rodent chow were significantly smaller than those to the consumption of sugar, chocolate, and peanut (Fig. 4D, E), in stark contrast to the similarity of STN responses to rodent chow and palatable foods in hungry mice (Fig. 3A, B). Thus, STN neurons may discriminate the palatability of food in sated mice.

Excitability of STN Neurons Differs Between Hungry and Sated Mice

To understand whether the more robust STN response to food consumption in the hungry than the sated state is associated with energy state-dependence of the excitability of the STN neurons, we performed patch-clamp recordings to measure spontaneous and evoked firing of STN neurons in brain slices. We found that the spontaneous firing rates of STN neurons were higher in hungry than in sated mice (Fig. 5A–C); in addition, the responses to depolarizing stimuli were greater in hungry than in sated mice (Fig. 5D–E). As illustrated in Fig. 5F, STN neurons in hungry mice showed lower input resistance than those in sated mice. This result supports the notion that the enhanced responses of STN neurons in hungry mice to depolarizing stimuli

may come from activation of ion channels contributing to neuronal excitability rather than the increase of membrane resistance. These results suggest that the attenuation of the STN responses to food consumption in sated mice relative to hungry mice is associated with lower excitability of STN neurons.

Modulation of Food Intake by STN Neurons in Light and Dark Phases

Our preceding data demonstrated that STN neurons represent food consumption. The data suggest that STN neurons are involved in feeding behaviors or are activated by feeding circuits or feeding-related hormones. To understand whether STN neurons regulate food intake, we used optogenetic techniques to bidirectionally modulate STN neurons and determined whether the modulations alter food intake (Fig. 6A, D, E). Our brain slice patch-clamp recording data demonstrated that virally transducing CaMKII-ChR2-eYFP and NpHR3.0-eYFP (left panels in Fig. 6B, C) in the STN allowed photo-stimulation (Fig. 6B, right panel) and photo-inhibition (Fig. 6C, right panel) of STN neurons, respectively.

After verifying the functionality of viral vectors, we photo-regulated STN neurons while measuring food intake in freely-behaving mice after overnight fasting or regular

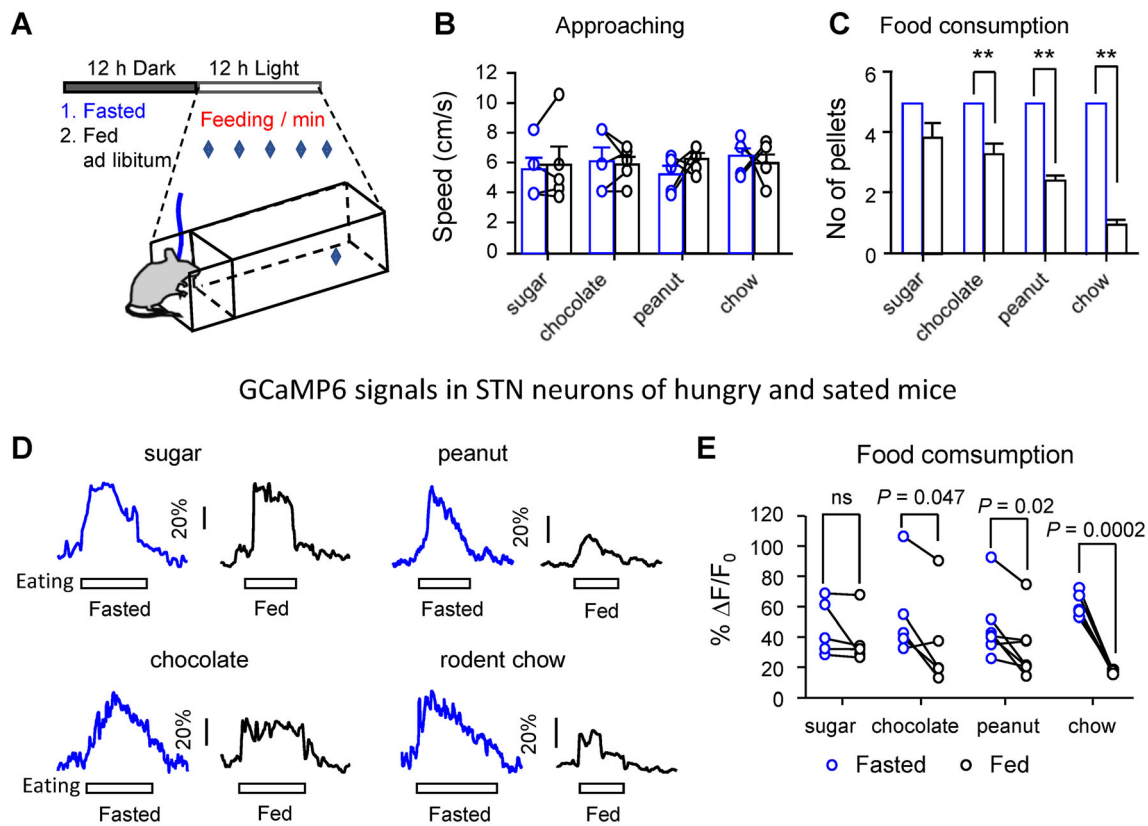


Fig. 4 STN responses to food intake decline with satiation. **A** Cartoon of protocol for satiation study. After overnight fasting or feeding *ad libitum*, mice were provided with food during the day. **B** Mice in hungry (blue) and sated (dark brown) states approached food pellets at similar speeds (sugar: $t = 0.31$, $P = 0.62$; chocolate: $t = 0.33$, $P = 0.75$; peanut: $t = 1.22$, $P = 0.29$; chow: $t = 0.42$, $P = 0.69$, $n = 5$, paired t -test). **C** Compared with hungry mice, sated mice ate fewer peanut pellets ($t = 14.55$, $P < 0.0001$, $n = 5$, paired t -test), chow pellets ($t = 24$, $P < 0.0001$, $n = 5$, paired t -test), and chocolate chunks ($t = 6.53$, $P = 0.003$, $n = 5$), but similar amounts of sugar ($t = 2.06$, $P = 0.11$, $n =$

5). **D**, **E** Typical traces (**D**) and summary (**E**) of responses of STN neurons to different foods in the day after overnight free access to food or overnight food deprivation (sugar, $t = 1.32$, $P = 0.26$, $n = 5$; chocolate, $t = 2.8$, $P = 0.047$, $n = 5$; peanut, $t = 3.02$, $P = 0.02$, $n = 7$; chow, $t = 12.25$, $P = 0.0002$, $n = 5$, paired t -test, fasted vs fed states). In the fed state, STN neurons responded differently to the consumption of different foods ($F = 4.90$, $P = 0.02$, two-way ANOVA; pairwise comparison: $t = 3.65$, $P = 0.01$, chow vs sugar; $t = 2.69$, $P = 0.039$, chow vs peanut; $t = 1.59$, $P = 0.138$, chow vs chocolate, Holm-Sidak method, $n = 5$).

feeding (Fig. 6D, E). We found that neither photo-stimulation (Fig. 6F) nor photo-inhibition (Fig. 6G) of STN neurons altered the 5-min food consumption after overnight fasting or regular feeding.

As the STN is involved in motor control [2, 3, 18, 42, 43], optogenetic modulation of STN neurons could alter movement, and subsequently interfere with food intake. To discriminate this confounding issue, we assessed the locomotor behavior while performing optogenetic regulation of STN neurons. We found that photo-stimulation of STN neurons reversibly enhanced the distance traveled per min in an open field by $\sim 50\%$ (Fig. 6H), while the motor effects of photo-inhibition were not statistically significant (Fig. 6I). Therefore, the regulation of food intake by optogenetic inhibition was not contaminated by altered locomotion.

As nocturnal animals, mice without fasting eat actively in the dark phase, but rarely in the light phase [44], we then

reversed light-dark cycle for at least 2 weeks, and measured 2-h food intake in the dark phase (Fig. 7A). After obtaining a stable baseline for at least 3 days, we applied optogenetic modulation to STN neurons (Fig. 7B). Photo-stimulation or photo-inhibition of STN neurons reduced (Fig. 7C) or increased (Fig. 7E) food intake, respectively. Note that photo-modulation of STN neurons significantly regulated food intake in the first hour, rather than the second hour (Fig. 7D, F), suggesting changes in the speed of eating. These results are similar to those of a previous study showing that a lesion in the STN increases food consumption in the first but not in the second hour [21].

These data indicate that stimulation of STN neurons reduces and inhibition of STN neurons increases food intake in the dark phase.

Our preceding data showed that STN neurons regulate food intake in the dark phase but not in the light phase. To

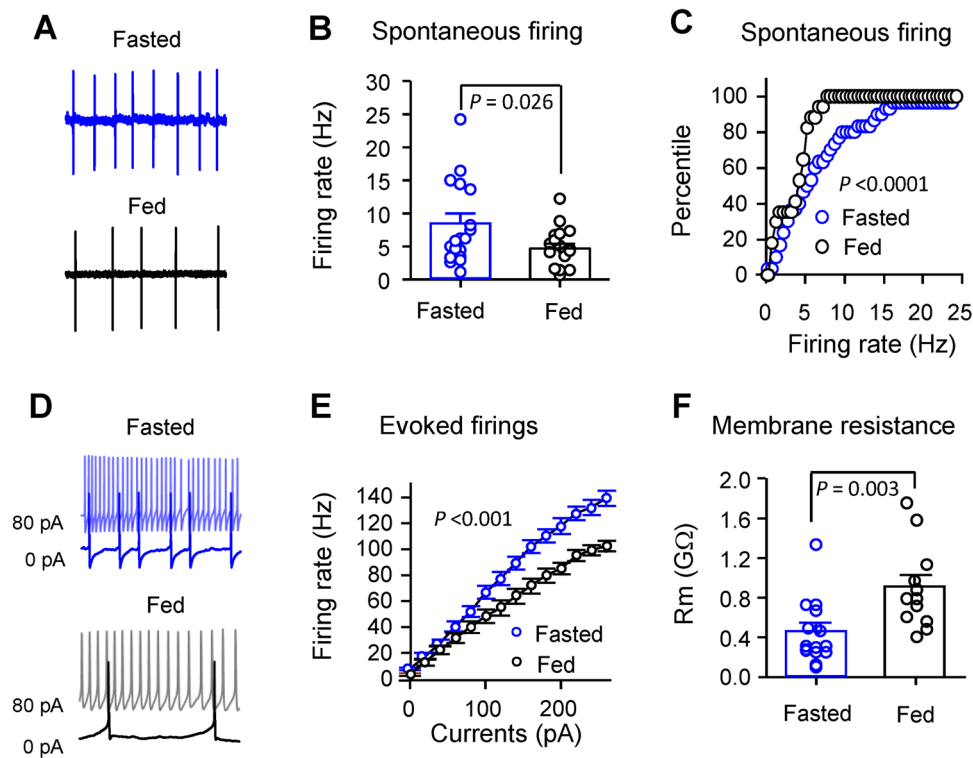


Fig. 5 Excitability of STN neurons differs between hungry and sated states. Cell-attached and whole-cell recordings were made from STN neurons in mice subjected to food deprivation (Fasted) and free access to food (Fed). **A–C** Typical traces of spontaneous firing (**A**), summary (**B**) (Fast: $n = 17$; Fed: $n = 18$; $t = 2.32$, $P = 0.026$, Student's t -test), and distribution (**C**) of spontaneous firing rate (Fast: $n = 17$; Fed: $n = 18$; statistics = 0.67, $P < 0.000001$, Kolmogorov-Smirnov test). **D** Typical traces of spontaneous (0 pA) and evoked (80 pA) firing from STN neurons in a fasted mouse (blue traces) and a fed mouse

(black traces). **E** Enhanced firing rates in response to depolarizing current (Fasted ($n = 17$) vs Fed ($n = 14$), $F = 13.77$, $P < 0.0001$; among currents (0–260 pA): $F = 433.5$, $P < 0.001$; interaction between Fast / Fed with Currents: $F = 13$, $P < 0.001$; two-way repeated measures ANOVA). **F** Membrane resistance measured as the response to a 5-mV hyperpolarizing voltage step from V_H (–50 mV) in STN neurons of fed ($n = 12$) and fasted mice ($n = 17$) ($t = 3.33$, $P = 0.003$, Student's t -test). These data were from 4 cage-mates: two were fed *ad libitum*, and two were subjected to 12–14 h of fasting.

determine the influence of light-dark cycle on STN responses to food intake, we performed fiber photometric recordings from freely behaving mice with AAV-CaMKII-GCaMP6S injection in the STN, and measured the responses of STN neurons to peanut pellet consumption in the light and dark phases (Fig. 8A–C). After 20 h food deprivation, the mice exhibited similar enhancement in the activity of STN neurons while the mice were consuming peanut pellets in the light and dark phases. These data suggest that STN responses to food intake may not change with the light-dark cycle.

Discussion

STN neurons are known to be involved in several behaviors, including movement, pain sensation, reward expectation, and reception [29–31, 45, 46]. In the present study, we showed that the activity of STN neurons exhibited a robust enhancement during the consumption of solid food, varying with physiological energy status of

the mice and the size, aversive flavor, and palatability of the food (Figs. 1, 4), and optogenetic modulation of STN neurons regulated food intake in the dark phase rather than the light phase (Figs. 6, 7). These results indicate that the STN represents and modulates food intake depending on internal physiological states and food properties.

Although the responses of STN neurons to drinking sweet and bitter liquids have been reported [29, 30, 45], no information is available about their responses to the consumption of solid food. Because the neural substrates mobilized by drinking and eating behaviors are different, at least in the sensory receptors [26, 47], STN neurons may differ in the responses to drinking and food intake. In the present study, we found that the activation of STN neurons by food consumption was enhanced (longer duration, but similar amplitude) when larger food pellets were ingested, but was reduced in both amplitude and duration when bitter food pellets were received. Breyse *et al.* demonstrated that the activity of STN neurons increases upon the reception of either sweet (sugar) or bitter (quinine) liquid, and the amplitude of the responses is augmented with more

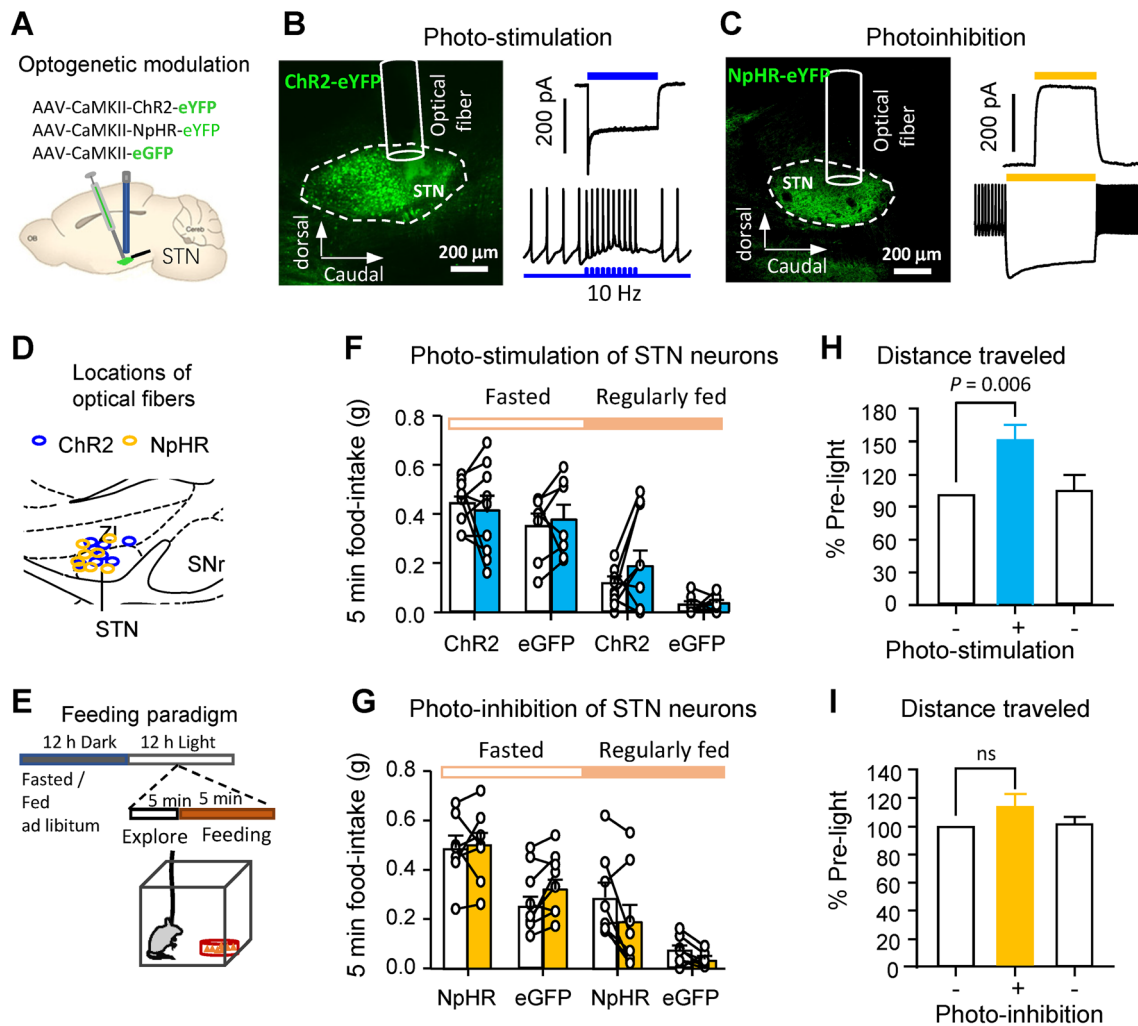


Fig. 6 Bidirectional optogenetic modulation of STN neurons does not change food intake in the light phase. **A** Cartoon of optogenetic modulation protocol. AAV-CaMKII-ChR2-eYFP (ChR2), AAV-CaMKII-NpHR3.0-eYFP (NpHR), or AAV-CaMKII-eGFP (eGFP) is injected into the STN and an optical fiber is implanted above the STN. **B** AAV-CaMKII-ChR2-eYFP is transduced into STN neurons (left panel), and blue light evokes an inward current in a voltage-clamped ($V_H = -50$ mV) STN neuron (upper right) and time-locked firing in a current-clamped STN neuron (lower right). **C** AAV-CaMKII-NpHR3.0-eYFP is efficiently transduced into STN neurons (left panel), and yellow light evokes an outward current in a voltage-clamped ($V_H = -50$ mV) STN neuron (upper right) and time-locked blocking of spontaneous firing in a current-clamped STN neuron (lower right). **D** Locations of optical fiber tips in the STN of mice in photo-inhibition experiments. **E** Cartoon of feeding protocol. After overnight fasting or regular feeding, each mouse is placed in a clean

cage in the day, allowed to habituate for 5 min, and then to consume food for 5 min. **F** Five-minute food intake in ChR2 and eGFP mice without (white bars) and with (blue bars) blue light stimulation (10 ms, 20 Hz, for 5 min) on two consecutive days (Fasted: ChR2, $n = 10$, $t = 1.19$, $P = 0.26$; Fasted: eGFP, $n = 7$, $t = 0.5$, $P = 0.62$; Fed: ChR2, $n = 10$, $t = 1.07$, $P = 0.31$; Fed: eGFP, $n = 7$, $t = 0.35$, $P = 0.74$). **G** In NpHR and eGFP mice, 5-min food intake without (white bars) and with (yellow bars) yellow light stimulation (5 min constant light) (Fasted: NpHR, $n = 8$, $t = 0.29$, $P = 0.78$; Fasted: eGFP, $n = 7$, $t = 2.04$, $P = 0.09$, paired t -test; Fed: NpHR, $n = 10$, $t = 2.41$, $P = 0.04$; Fed: eGFP, $n = 7$, $t = 1.87$, $P = 0.11$, paired t -test). In **F** and **G**, each open circle represents a data point from one mouse. The data points from the same mouse in two different conditions are connected with a line. **H–I** Modulation of locomotion by optogenetic stimulation (**H**, blue) ($n = 7$, $t = 5.31$, $P = 0.006$, paired t -test) and inhibition (**I**, yellow) ($n = 7$, $t = 2.20$, $P = 0.08$, paired t -test).

concentrated sugar solutions [30]. These results suggest that STN neurons may encode the relative size and valence of food with a pattern different from the concentration and valence of liquid [30].

The pattern of STN responses to food consumption also differs from that of midbrain DA neurons to reward magnitude and valence [48, 49]. First, midbrain DA

neurons discriminate the magnitude of a reward by recognizing the difference between the encountered and experienced reward: enhancing activity upon a better reward, but suppressing activity upon a worse one. Second, midbrain DA neurons display opposite responses to rewarding and aversive stimulation.

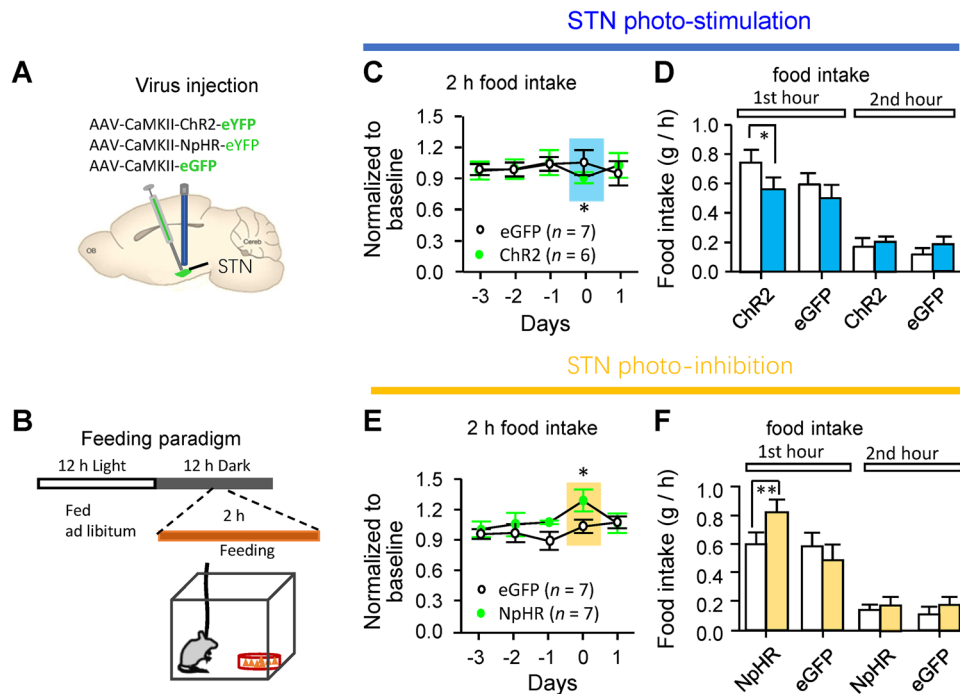


Fig. 7 Bidirectional optogenetic modulation of STN neurons alters food intake in the dark phase. **A** Cartoon of the virus injection protocol. AAV-CaMKII-ChR2-eYFP (ChR2), AAV-CaMKII-NpHR3.0-eYFP (NpHR), or AAV-CaMKII-eGFP (eGFP) was injected into the mouse STN and an optical fiber was implanted above the STN. **B** Cartoon of the feeding paradigm. The mice were provided with rodent chow in the light phase, but deprived of food in the dark phase; 2-h food-intake was measured in the dark phase. **C–F** After a stable baseline was obtained for at least 3 days, 2-min episodes of blue light (20 Hz, 10 ms) separated by 2-min intervals were delivered into the STN of ChR2 and eGFP mice (**C, D**; ChR2: $n = 6$, $t = 3.82$, $P = 0.02$, paired t -test; eGFP: $n = 7$, $t = 0.16$, $P = 0.88$,

paired t -test; day 0 vs day -1), or 2-min episodes of yellow light (constant) separated by 2-min intervals were delivered into the STN of NpHR and eGFP mice (**E, F**; NpHR: $n = 7$, $t = 2.88$, $P = 0.03$; eGFP: $n = 7$, $t = 0.16$, $P = 0.88$, paired t -test; day 0 vs day -1). Photo-stimulation (**D**) of STN neurons reduced and photo-inhibition (**F**) increased the food intake in the first hour (ChR2: $n = 6$, $t = 3.44$, $P = 0.02$; eGFP-blue light: $n = 7$, $t = 0.12$, $P = 0.91$; NpHR: $n = 7$, $t = 3.55$, $P = 0.01$; eGFP-yellow light: $n = 7$, $t = 0.20$, $P = 0.85$, paired t -test), but not in the second hour (ChR2: $n = 6$, $t = 0.48$, $P = 0.65$; eGFP-blue light: $n = 7$, $t = 1.09$, $P = 0.32$; NpHR: $n = 7$, $t = 0.58$, $P = 0.58$; eGFP-yellow light: $n = 7$, $t = 1.55$, $P = 0.17$, paired t -test).

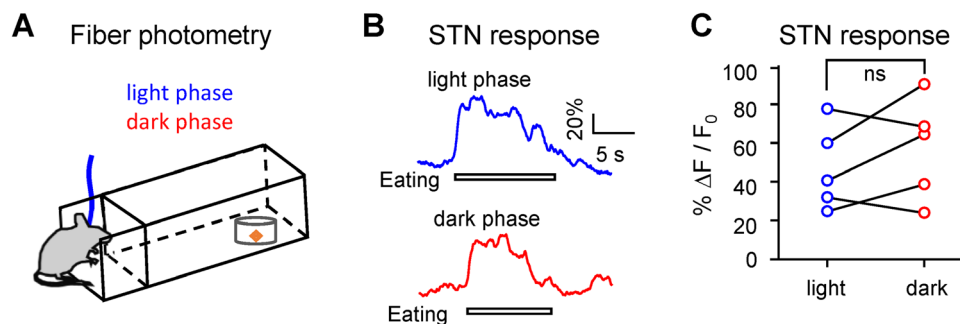


Fig. 8 Representation of feeding is not altered in the dark phase. **A** Fiber photometry was performed in mice injected with AAV-CaMKII-GCaMP6S into the STN during feeding in the light and dark phases. Food was deprived for 20 h before tests in both situations.

B Typical traces showing STN responses while a mouse was eating a peanut pellet in either the light (blue) or dark phase (red). **C** STN responses of 5 mice to feeding in the light (blue) and dark (red) phases ($t = 1.26$, $P = 0.28$, $n = 5$, paired t -test).

Previous electrophysiological studies have shown that the activity of STN neurons is enhanced upon drinking [30], but did not address whether the action of drinking or eating without the reception of water or food could activate STN neurons. We recorded smaller STN responses to the execution of eating and drinking (without procurement of

food and water) than those to their successful acquisition (Fig. 2). This set of experiment suggests that STN neurons may encode both the action and outcome evaluation of feeding and drinking behaviors.

Pavlovian conditioning has been used to address the involvement of STN neurons in processing the liquid

reward [29, 30, 45]. It was unknown whether STN neurons can be differentially activated in sated and hungry mice. We found that STN neurons responded less robustly to food consumption (rodent chow, peanut, and chocolate) when the mice were sated than when they were hungry (Fig. 4). Our electrophysiological data suggest that the effect of energy deficiency on STN responses to food may be related to the enhanced excitability of STN neurons. Further investigations are warranted to elucidate whether STN neurons are directly or indirectly regulated by hunger- or satiation-related hormones.

A previous study has shown that STN neurons respond similarly when a monkey chooses to drink water and sweet liquid [45]. It seems that monkey STN neurons do not discriminate between high (sweet liquid) and low (water) rewards. In contrast, rat STN neurons show enhanced activation in response to a high concentration, relative to a low concentration of sugar [30]. In mice, rodent chow may have a low value, and palatable food a high reward value. We demonstrated that STN neurons are able to discriminate the palatability of food in sated mice (Fig. 3), but not in hungry mice (Fig. 2). Therefore, STN responses to food consumption are determined by species, reward values, and energy homeostatic status.

It has been demonstrated that either STN DBS or lesions of the STN increase food intake or the motivation for food [20, 21, 50]. In these studies, DBS recruits neighboring neurons and efferent, afferent, and/or *en passant* axons (including both excitatory and inhibitory fibers) and lesions of STN neurons are irreversible. In these scenarios, the consistent stimulation or inhibition of STN neurons without neuroadaptation may not be achieved. To overcome these limitations, we performed bidirectional optogenetic modulation of STN neurons. Interestingly, in the light phase, optogenetic modulation of STN neurons did not alter food intake in either hungry or sated mice, while in the dark phase, stimulation of STN neurons reduced and inhibition of STN neurons increased food intake. We argue that in the light phase, food intake may strongly rely on energy homeostasis, and STN neurons may lack the ability to alter this internal drive. On the contrary, in the dark phase, food intake may be initiated under a natural drive, and modulation of STN neurons significantly alters food intake. These data suggest that the STN regulates food intake only when synchronized with the natural drive for food.

We demonstrated that STN neurons in hungry mice showed enhanced excitability and stronger responses to food consumption than those in sated mice (Fig. 3). These data support the hypothesis that the excitability of STN neurons is promoted by hunger hormones but inhibited by satiation hormones. Further investigations are needed to test this. Our data also suggest that STN responses to feeding may be relevant to the motivation for food, and

increasing firing rates in STN neurons with optogenetics increases food intake. Surprisingly, in our optogenetic experiments, we found that photostimulation of STN neurons reduced food intake in the dark phase (Fig. 7). Regarding this inconsistency, we argue that the excitation of STN neurons during food consumption could result from the regulation of STN neurons by feeding circuits, but the alteration of food intake after optogenetic modulation of the STN could be a consequence of the regulation of feeding circuits by STN neurons. These two processes may mobilize a distinct repertoire of hormones and brain regions. We found that STN responses to feeding in the light and dark phases were similar (Fig. 8A-C), suggesting that the feeding circuits, when activated, stimulate the STN. However, the regulation of feeding circuits by the STN may depend on the timing of the natural drive for food. Further investigations are warranted to address reciprocal interactions between the STN and the feeding circuits in different physiological states.

In summary, we reveal that STN neurons are involved in feeding behavior and regulate food intake. Briefly, the overall activity of STN neurons was enhanced in response to food consumption depending on the size, valence, and palatability of food and the physiological status of the animals; stimulation of STN neurons reduced food intake, while the suppression of STN neurons promoted food intake. As STN DBS inhibits neuronal activity in a considerable proportion of STN neurons [2, 18], we propose that increasing food intake through inhibition of STN neurons could be a physiological mechanism underlying the weight gain following STN DBS. Future studies are needed to further dissect the STN circuits that separately control motor and feeding behaviors to precisely restore motor function but avoid weight gain in the treatment of PD patients with STN DBS.

Acknowledgements This work was supported by the National Natural Science Foundation of China (81701100, 81870891, and 81971038), the Fund for Jiangsu Province Specially-Appointed Professor (2016 and 2018), the Natural Science Foundation of Jiangsu Province, China (BK20171160), the Natural Science Foundation of the Jiangsu Higher Education Institutions of China (17KJA320007 and 18KJA320009), the Jiangsu Province Fund for Dominant Discipline (Anesthesiology), and Academic Startup Packages from Xuzhou Medical University, China (D2017009 and D2017010).

Conflict of interest The authors declare that there are no conflicts of interest.

References

1. Faggiani E, Benazzouz A. Deep brain stimulation of the subthalamic nucleus in Parkinson's disease: From history to the interaction with the monoaminergic systems. *Prog Neurobiol* 2017, 151: 139–156.

2. Hamani C, Florence G, Heinsen H, Plantinga BR, Temel Y, Uludag K, *et al.* Subthalamic nucleus deep brain stimulation: Basic concepts and novel perspectives. *eNeuro* 2017, 4: ENEURO.0140–17.2017.
3. Chen X, Zhang C, Li Y, Huang P, Lv Q, Yu W, *et al.* Functional connectivity-based modelling simulates subject-specific network spreading effects of focal brain stimulation. *Neurosci Bull* 2018, 34: 921–938.
4. Bannier S, Montaurier C, Derost PP, Ulla M, Lemaire JJ, Boirie Y, *et al.* Overweight after deep brain stimulation of the subthalamic nucleus in Parkinson disease: long term follow-up. *J Neurol Neurosurg Psychiatry* 2009, 80: 484–488.
5. Foubert-Samier A, Maurice S, Hivert S, Guelh D, Rigalleau V, Burbaud P, *et al.* A long-term follow-up of weight changes in subthalamic nucleus stimulated Parkinson's disease patients. *Rev Neurol (Paris)* 2012, 168: 173–176.
6. Montaurier C, Morio B, Bannier S, Derost P, Arnaud P, Brandolini-Bunlon M, *et al.* Mechanisms of body weight gain in patients with Parkinson's disease after subthalamic stimulation. *Brain* 2007, 130: 1808–1818.
7. Kistner A, Lhomme E, Krack P. Mechanisms of body weight fluctuations in Parkinson's disease. *Front Neurology* 2014, 5: 84.
8. Witjas T, Baunez C, Henry JM, Delfini M, Regis J, Cherif AA, *et al.* Addiction in Parkinson's disease: Impact of subthalamic nucleus deep brain stimulation. *Mov Disord* 2005, 20: 1052–1055.
9. Balestrino R, Baroncini D, Fichera M, Donofrio CA, Franzin A, Mortini P, *et al.* Weight gain after subthalamic nucleus deep brain stimulation in Parkinson's disease is influenced by dyskinesias' reduction and electrodes' position. *Neurol Sci* 2017, 38: 2123–2129.
10. Millan SH, Hacker ML, Turchan M, Molinari AL, Currie AD, Charles D. Subthalamic nucleus deep brain stimulation in early stage Parkinson's disease is not associated with increased body mass index. *Parkinsons Dis* 2017, 2017: 7163801.
11. Markaki E, Ellul J, Kefalopoulou Z, Trachani E, Theodoropoulou A, Kyriazopoulou V, *et al.* The role of ghrelin, neuropeptide Y and leptin peptides in weight gain after deep brain stimulation for Parkinson's disease. *Stereotact Funct Neurosurg* 2012, 90: 104–112.
12. Novakova L, Ruzicka E, Jech R, Serranova T, Dusek P, Urgosik D. Increase in body weight is a non-motor side effect of deep brain stimulation of the subthalamic nucleus in Parkinson's disease. *Neuro Endocrinol Lett* 2007, 28: 21–25.
13. Ruzicka E, Novakova L, Jech R, Urgosik D, Ruzicka F, Haluzik M. Decrease in blood cortisol corresponds to weight gain following deep brain stimulation of the subthalamic nucleus in Parkinson's disease. *Stereotact Funct Neurosurg* 2012, 90: 410–411.
14. Ruzicka F, Jech R, Novakova L, Urgosik D, Bezdicek O, Vymazal J, *et al.* Chronic stress-like syndrome as a consequence of medial site subthalamic stimulation in Parkinson's disease. *Psychoneuroendocrinology* 2015, 52: 302–310.
15. Ruzicka F, Jech R, Novakova L, Urgosik D, Vymazal J, Ruzicka E. Weight gain is associated with medial contact site of subthalamic stimulation in Parkinson's disease. *PLoS One* 2012, 7: e38020.
16. Novakova L, Haluzik M, Jech R, Urgosik D, Ruzicka F, Ruzicka E. Hormonal regulators of food intake and weight gain in Parkinson's disease after subthalamic nucleus stimulation. *Neuro Endocrinol Lett* 2011, 32: 437–441.
17. Seifried C, Boehncke S, Heinzmann J, Baudrexel S, Weise L, Gasser T, *et al.* Diurnal variation of hypothalamic function and chronic subthalamic nucleus stimulation in Parkinson's disease. *Neuroendocrinology* 2013, 97: 283–290.
18. Gradinaru V, Mogri M, Thompson KR, Henderson JM, Deisseroth K. Optical deconstruction of parkinsonian neural circuitry. *Science* 2009, 324: 354–359.
19. Barutca S, Turgut M, Meydan N, Ozsunar Y. Subthalamic nucleus tumor causing hyperphagia—case report. *Neurol Med Chir (Tokyo)* 2003, 43: 457–460.
20. Etemadifar M, Abtahi SH, Abtahi SM, Mirdamadi M, Sajjadi S, Golabbakhsh A, *et al.* Hemiballismus, hyperphagia, and behavioral changes following subthalamic infarct. *Case Rep Med* 2012, 2012: 768580.
21. Baunez C, Amalric M, Robbins TW. Enhanced food-related motivation after bilateral lesions of the subthalamic nucleus. *J Neurosci* 2002, 22: 562–568.
22. Baunez C, Dias C, Cador M, Amalric M. The subthalamic nucleus exerts opposite control on cocaine and 'natural' rewards. *Nat Neurosci* 2005, 8: 484–489.
23. Kenny PJ. Reward mechanisms in obesity: new insights and future directions. *Neuron* 2011, 69: 664–679.
24. Bojanowska E, Ciosek J. Can we selectively reduce appetite for energy-dense foods? An overview of pharmacological strategies for modification of food preference behavior. *Curr Neuropharmacol* 2016, 14: 118–142.
25. Fang PH, Yu M, Ma YP, Li J, Sui YM, Shi MY. Central nervous system regulation of food intake and energy expenditure: role of galanin-mediated feeding behavior. *Neurosci Bull* 2011, 27: 407–412.
26. Schwartz GJ, Zeltser LM. Functional organization of neuronal and humoral signals regulating feeding behavior. *Annu Rev Nutr* 2013, 33: 1–21.
27. Sternson SM, Eiselt AK. Three pillars for the neural control of appetite. *Annu Rev Physiol* 2017, 79: 401–423.
28. Berridge KC. Food reward: Brain substrates of wanting and liking. *Neurosci Biobehav Rev* 1996, 20: 1–25.
29. Darbaky Y, Baunez C, Arecchi P, Legallet E, Apicella P. Reward-related neuronal activity in the subthalamic nucleus of the monkey. *Neuroreport* 2005, 16: 1241–1244.
30. Breyse E, Pelloux Y, Baunez C. The good and bad differentially encoded within the subthalamic nucleus in rats. *eNeuro* 2015, 2: ENEURO.0014-0015.2015.
31. Rossi PJ, Gunduz A, Okun MS. The subthalamic nucleus, limbic function, and impulse control. *Neuropsychol Rev* 2015, 25: 398–410.
32. Cho JR, Treweek JB, Robinson JE, Xiao C, Bremner LR, Greenbaum A, *et al.* Dorsal raphe dopamine neurons modulate arousal and promote wakefulness by salient stimuli. *Neuron* 2017, 94: 1205–1219.e8.
33. Xiao C, Cho JR, Zhou C, Treweek JB, Chan K, McKinney SL, *et al.* Cholinergic mesopontine signals govern locomotion and reward through dissociable midbrain pathways. *Neuron* 2016, 90: 333–347.
34. Xiao C, Miwa JM, Henderson BJ, Wang Y, Deshpande P, McKinney SL, *et al.* Nicotinic receptor subtype-selective circuit patterns in the subthalamic nucleus. *J Neurosci* 2015, 35: 3734–3746.
35. Zhou C, Gu W, Wu H, Yan X, Deshpande P, Xiao C, *et al.* Bidirectional dopamine modulation of excitatory and inhibitory synaptic inputs to subthalamic neuron subsets containing alpha4-beta2 or alpha7 nAChRs. *Neuropharmacology* 2019, 148: 220–228.
36. Zhong W, Li Y, Feng Q, Luo M. Learning and stress shape the reward response patterns of serotonin neurons. *J Neurosci* 2017, 37: 8863–8875.
37. Sun C, Tang K, Wu J, Xu H, Zhang W, Cao T, *et al.* Leptin modulates olfactory discrimination and neural activity in the olfactory bulb. *Acta Physiol (Oxf)* 2019, 227: e13319.

38. Wang D, Liu P, Mao X, Zhou Z, Cao T, Xu J, *et al.* Task-demand-dependent neural representation of odor information in the olfactory bulb and posterior piriform cortex. *J Neurosci* 2019, 39: 10002–10018.
39. Wang D, Wang X, Liu P, Jing S, Du H, Zhang L, *et al.* Serotonergic afferents from the dorsal raphe decrease the excitability of pyramidal neurons in the anterior piriform cortex. *Proc Natl Acad Sci U S A* 2020, 117: 3239–3247.
40. Noldus LP, Spink AJ, Tegelenbosch RA. EthoVision: a versatile video tracking system for automation of behavioral experiments. *Behav Res Methods Instrum Comput* 2001, 33: 398–414.
41. Schneider CA, Rasband WS, Eliceiri KW. NIH Image to ImageJ: 25 years of image analysis. *Nat Methods* 2012, 9: 671–675.
42. Benarroch EE. Subthalamic nucleus and its connections: Anatomic substrate for the network effects of deep brain stimulation. *Neurology* 2008, 70: 1991–1995.
43. Wang Y, Wang Y, Liu J, Wang X. Electroacupuncture alleviates motor symptoms and up-regulates vesicular glutamatergic transporter 1 expression in the subthalamic nucleus in a unilateral 6-hydroxydopamine-lesioned hemi-Parkinsonian rat model. *Neurosci Bull* 2018, 34: 476–484.
44. Espinosa-Carrasco J, Burokas A, Fructuoso M, Erb I, Martin-Garcia E, Gutierrez-Martos M, *et al.* Time-course and dynamics of obesity-related behavioral changes induced by energy-dense foods in mice. *Addict Biol* 2018, 23: 531–543.
45. Espinosa-Parrilla JF, Baunez C, Apicella P. Modulation of neuronal activity by reward identity in the monkey subthalamic nucleus. *Eur J Neurosci* 2015, 42: 1705–1717.
46. Pautrat A, Rolland M, Barthelemy M, Baunez C, Sinniger V, Piallat B, *et al.* Revealing a novel nociceptive network that links the subthalamic nucleus to pain processing. *Elife* 2018, 7: e36607.
47. Ryan PJ. The Neurocircuitry of fluid satiation. *Physiol Rep* 2018, 6: e13744.
48. Matsumoto H, Tian J, Uchida N, Watabe-Uchida M. Midbrain dopamine neurons signal aversion in a reward-context-dependent manner. *Elife* 2016, 5: e17328.
49. Cohen JY, Haesler S, Vong L, Lowell BB, Uchida N. Neuron-type-specific signals for reward and punishment in the ventral tegmental area. *Nature* 2012, 482: 85–88.
50. Serranova T, Jech R, Dusek P, Sieger T, Ruzicka F, Urgosik D, *et al.* Subthalamic nucleus stimulation affects incentive salience attribution in Parkinson's disease. *Mov Disord* 2011, 26: 2260–2266.